Lysophosphatidic Acid Receptor Signaling in Mammalian Retinal Pigment Epithelial Cells

Wallace B. Thoreson,[1,2] Jennifer S. Ryan,[3] Chanjuan Shi,[3] Melanie E. Kelly,[3,4] Eric J. Bryson,[1] Myron L. Toews,[2] Tracy L. Ediger,[2] and David M. Chacko[1]

Purpose. Lysophosphatidic acid (LPA) is a phospholipid growth factor that stimulates proliferation, chemotaxis, cation currents, and K^+ currents in retinal pigment epithelial (RPE) cells. LPA receptor transduction was analyzed in human and rat RPE cells.

Methods. Cells were cultured with standard methods, and signaling pathways were analyzed with a variety of approaches, including whole-cell recording, calcium imaging, and second-messenger assays.

Results. LPA-activated nonselective cation currents in rat RPE were blocked by the protein tyrosine kinase (PTK) inhibitor genistein, by the MAP kinase kinase (MEK) inhibitor PD98059, and by loading cells with antibodies to $G_{\alpha i/o/t/z}$. LPA activated the MAP kinase and extracellular signal-related kinase (ERK)-1, and produced a dose-dependent inhibition of cAMP production. LPA stimulated a dose-dependent increase in $[Ca^{2+}]_i$ that persisted in Ca^{2+}-free medium and was reduced by pretreatment with thapsigargin, suggesting it involves release from intracellular stores. The $[Ca^{2+}]_i$ increase was not blocked by ryanodine or the phospholipase C inhibitor U73122. LPA did not stimulate inositol phosphate production. Similar to the cation current, LPA-evoked $[Ca^{2+}]_i$ increases were blocked by PD98059 and by loading cells with antibodies to $G_{\alpha i/o/t/z}$. RT-PCR experiments showed the presence of RNA for three LPA receptor subtypes (Edg2, -4, and -7); RNase protection assays showed the strongest expression for Edg2 receptor RNA.

Conclusions. LPA receptors in RPE cells activate pertussis toxin (PTx)-sensitive G proteins that inhibit cAMP accumulation; stimulate MAP kinase which activates a cation current and probably contributes to mitogenesis; and stimulate release of Ca^{2+} from intracellular stores that appears independent of IP_3 and ryanodine receptor activation. (*Invest Ophthalmol Vis Sci.* 2002;43:2450–2461)

From the Departments of [1]Ophthalmology and [2]Pharmacology, University of Nebraska Medical Center, Omaha, Nebraska; and the Departments of [3]Pharmacology and [4]Ophthalmology, Dalhousie University, Halifax, Nova Scotia, Canada.

Supported by a Fight for Sight Grant-in-Aid (DMC), a University of Nebraska Medical Center Seed Grant (DMC), Nebraska Lion's Eye Institute (DMC, WBT), the Gifford Foundation (DMC, WBT), a Research to Prevent Blindness Career Development Award (WBT), National Eye Institute Grant EY10542 (WBT), and the National Science and Engineering Council (NSERC) of Canada (MEK, JSR).

Submitted for publication August 8, 2001; revised January 28, 2002; accepted March 1, 2002.

Commercial relationships policy: N.

The publication costs of this article were defrayed in part by page charge payment. This article must therefore be marked "*advertisement*" in accordance with 18 U.S.C. §1734 solely to indicate this fact.

Corresponding author: Wallace B. Thoreson, Department of Ophthalmology, 985540 Nebraska Medical Center, University of Nebraska Medical Center, Omaha, NE 68198-5540; wbthores@unmc.edu.

Lysophosphatidic acid (LPA) is one of a family of phospholipid growth factors that mediate diverse biological activities, including cell proliferation, inhibition of apoptosis, regulation of growth factor expression, and cytoskeletal rearrangement (for reviews, see Refs. 1–4). LPA is released from activated platelets, injured cells, and growth factor–stimulated cells and is present in activated serum at levels of 5 to 25 μM.[5] The actions of LPA and related phospholipid growth factors (e.g., sphingosine-1-phosphate) account for much of the biological activity of serum.[1] LPA is also present in other biological fluids, including aqueous humor, lacrimal gland fluid, and ascitic fluid of patients with ovarian cancer.[6,7]

Biological effects of LPA have received relatively little attention in ocular tissues. In corneal keratocytes, LPA can stimulate Cl^- currents[8] and cell contraction[9] and, in corneal epithelium, LPA sensitizes Ca^{2+} influx through mechanosensitive channels[10] and stimulates cell migration.[11] In retina, LPA stimulates intracellular Ca^{2+} increases in chick retinal neurons[12] and both cation and K^+ currents in Müller cells and retinal pigment epithelial (RPE) cells.[13,14] In RPE cells, LPA also stimulates cell proliferation and chemotaxis.[15] The proliferative and chemotactic effects of LPA in RPE cells, along with LPA's ability to stimulate fibroblast contraction,[9] suggest that the LPA, which is present in activated serum, may contribute to development of epiretinal membranes during proliferative vitreoretinopathy.

In the present study, we investigated the signal transduction mechanisms of LPA receptors in mammalian RPE cells. The actions of LPA are mediated by G-protein–coupled receptors that can couple to a variety of signaling pathways.[1,2] A family of phospholipid growth factor receptors has been cloned,[16–23] including three subtypes (Edg2, -4, and -7) that are selectively activated by LPA. LPA's activation of G_i proteins leads to inhibition of cAMP production and stimulation of proliferation by mitogen-activated protein kinase (MAPK), as well as stimulation of phospholipase C activity in some cells. Activation of G_q leads to stimulation of phospholipase C activity, and activation of $G_{12/13}$ by LPA can stimulate the small guanosine triphosphatase (GTPase) Rho.[1,2] In studies of RPE cells, investigators have found that the LPA-evoked cation current and proliferation are inhibited by pertussis toxin (PTx), suggesting that the LPA receptor transduction cascade involves PTx-sensitive G proteins.[15,24] A PTx-sensitive cation current that is modulated by MAPK phosphorylation has been previously described in RPE cells, prompting the hypothesis that LPA-evoked cation current may be modulated by MAPK signaling pathways.[25,26] In the results of the present study, LPA receptors in RPE cells coupled to PTx-sensitive G proteins to inhibit accumulation of cAMP and stimulate MAPK, which in turn regulated a cation current. Activation of PTx-sensitive G proteins by LPA also stimulated a release of Ca^{2+} from intracellular stores that appeared independent of activation of IP_3 and ryanodine receptor.

Methods

Cell Dissociation and Culture of Rat RPE Cells

Long-Evans rats (postnatal age, 8–14 days) were anesthetized using halothane, killed by decapitation, and the eyes enucleated. All proce-

Investigative Ophthalmology & Visual Science, July 2002, Vol. 43, No. 7

dures were performed in accordance with the ARVO Statement for the Use of Animals in Ophthalmic and Vision Research. RPE cells were isolated with a modification of the method of Wang et al.[27] Enucleated eyes were placed in Ca^{2+}-free Hanks' solution containing EDTA (CFHE; Life Technologies, Burlington, Ontario, Canada). The connective tissue was removed, and the globes bisected along the equator just posterior to the ora serrata, leaving the neural retina attached to the posterior eyecup. The anterior portion of the eye containing the cornea, lens, and vitreous was discarded. The posterior eyecup was then placed in CFHE containing 220 U/mL hyaluronidase type III (Sigma Chemical Co., St. Louis, MO) and 65 U/mL collagenase A (Roche Molecular Biochemicals, Indianapolis, IN) for 10 minutes at 37°C. Under a dissecting microscope, in fresh CFHE without enzyme, the neural retina was gently peeled from the eyecup with forceps. The remaining posterior segment was incubated at 37°C for 5 minutes in CFHE enzyme solution to facilitate dissociation of the RPE from the Bruch's membrane. After a second transfer to fresh CFHE, sheets of RPE cells were gently removed from the remaining eyecup with forceps, to avoid disturbing the underlying choroid. RPE tissue was triturated through a narrow-bore, fire-polished Pasteur pipette, to yield a suspension of single cells and small clumps of RPE tissue. The cell suspension was washed and resuspended in 500 μL Dulbecco's modified Eagle's medium (DMEM) plus 20% fetal calf serum (FCS), 0.5% penicillin-streptomycin, and gentamicin (50 μg/mL; Sigma Chemical Co.). For electrophysiological recording, RPE cells were seeded onto glass coverslips (12 mm diameter) in four-well culture dishes for 2 to 5 days. For Western blot analysis, RPE cells were plated into 7-mL tissue culture flasks or six-well culture plates and grown to confluence ($\sim 10^6$ cells/mL). The medium was changed to DMEM containing 10% FCS and antibiotics 24 hours after the initial plating. Cells were maintained in a 37°C incubator with 5% CO_2.

Cell Dissociation and Culture of Human RPE Cells

Human eyes were obtained from the Nebraska Lion's Eye Bank within 15 hours of death. Acceptable eyes were aseptic with no history of retinal disease and no gross abnormalities. Eyes of donors with human immunodeficiency virus (HIV) or hepatitis C were also excluded. These studies were conducted according to the provisions of the Declaration of Helsinki for experiments involving human tissue.

After removing the anterior segment, lens, vitreous, and neural retina, the RPE cells were enzymatically dissociated from the eyecup by using two successive treatments (20 and 30 minutes) of trypsin (0.05% trypsin, 0.53 mM EDTA, Ca- and Mg-free). Cells were then washed twice with RPE growth medium (DMEM supplemented with 10% FCS, MEM nonessential amino acids, and 10 μg/mL gentamicin) and plated. Cells were fed RPE growth medium twice weekly and incubated in a moist incubator at 37°C with 5% CO_2. Cells were subcultured after reaching confluence. Cells of passages 2 through 6 were used in the present study.

Mammalian RPE cells in culture initially contain melanin granules, exhibit typical epithelial cell morphology, and can be labeled with a monoclonal antibody to cytokeratin (mAb 8.13) or an antibody specific for RPE cells (RET-PE2).[20,28]

G Protein α Subunit Antibody Loading Technique

RPE cells were loaded with antibodies against G_α subunits as described by Ryan and Kelly.[26] Briefly, cells grown for 3 to 5 days in culture were incubated with trypsin-EDTA for 5 minutes and then washed with an excess of DMEM. The cells were then centrifuged at 5000*g* for 5 minutes, washed, resuspended, and plated in 250 μL DMEM-10% FCS containing 25 μL $G_{\alpha i/o/t/z}$ antiserum solution (100 μg/mL; Santa Cruz Biotechnology, Santa Cruz, CA) to give a final antibody concentration of 10 μg/mL. Resuspended cells were allowed to replate onto glass coverslips for 12 to 14 hours in the incubator. Cells from the same culture resuspended in the absence of antisera were used as the control. Efficiency of antibody incorporation in this method typically appeared to be more than 90%, as observed by positive staining with a goat anti-rabbit secondary antibody conjugated to FITC (data not shown).

Solutions for Electrophysiological Experiments

RPE cells attached to glass coverslips were placed in a shallow recording chamber (volume, ~1 mL) and positioned on the stage of an inverted microscope (Nikon Instruments, Melville, NY). The recording chamber was superfused (1–2 mL/min) with a variety of solutions by gravity inflow from elevated reservoirs. The flow rate was regulated by a series of valves. All extracellular and intracellular solutions were adjusted to pH 7.3 to 7.4, and the osmolarity was measured by freezing point depression (Osmette A; Fischer Scientific, Fairlawn, NJ). Extracellular solutions had a final osmolarity of 330 to 340 mOsM, and the osmolarity of intracellular solutions was between 310 and 320 mOsM. The use of a slightly hyperosmotic external solution was found to be effective in eliminating transient changes in ionic conductances, which occurred as a result of osmotic changes during the initial period of whole-cell recording. The standard extracellular solution contained (in mM): NaCl, 130; KCl, 5; Na-HEPES, 10; $NaHCO_3$, 10; $MgCl_2$, 1; $CaCl_2$, 1; and glucose, 10. The standard low-Cl^- intracellular solution contained (in mM): K-aspartate, 100; KCl, 10; HEPES acid, 20; $MgCl_2$, 1; $CaCl_2$, 0.4; EGTA, 1; adenosine triphosphate (ATP), 1; and GTP, 0.1. For experiments in which K^+ currents were minimized, KCl in the standard external solution was replaced with 5 mM tetraethylammonium chloride (TEACl), and K-aspartate in the internal solution was replaced with 100 mM Cs-aspartate.

A stock solution of LPA (10 mM 1-oleoyl LPA in 0.25% fatty-acid–depleted bovine serum albumin) was diluted in the extracellular recording solution and applied by pressure injection from a micropipette. Micropipettes with tips approximately 2 μm in diameter were positioned 50 to 100 μm from the cells and 14 to 34 kPa (2–5 lb/in.^{2}) pressure was applied to the back of the micropipettes (Picospritzer II; General Valve Corp., Fairfield, NJ). Cells were preincubated (20 minutes) and bath perfused for a minimum of 5, usually 10, complete (1 mL) bath exchanges in experiments with the inhibitors genistein, daidzein, or PD98059 diluted into the extracellular recording solution.

Electrophysiological Recordings in Rat RPE Cells

The whole-cell patch–clamp technique was used to measure currents in isolated rat RPE cells.[29] Patch electrodes were pulled from borosilicate glass micropipettes (1.5 μm outer diameter, 1.1 μm inner diameter; Sutter Instruments, San Raphael, CA), with a two-stage vertical microelectrode puller (model PP83; Narishige USA, Greenvale, NY). Electrodes were coated with beeswax to reduce input capacitance[30] and had resistances of 2 to 3 MΩ when filled with intracellular solution and placed in the extracellular bathing solution. The reference electrode used was a sealed electrode-salt bridge combination (Dri-Ref-2; World Precision Instruments, Sarasota, FL). Offset potentials were nullified using the amplifier circuitry before seals were made on cells. All the data and current–voltage (I-V) relationships shown have been corrected for liquid junction potentials (LJPs) arising between the bath and the electrode.[31] LJPs were measured experimentally and were also calculated using a software program (JPCalc, ver. 2.00; P. H. Barry, Sydney, Australia). LJPs were defined as the potential of the bath solution with respect to the pipette solution. For whole-cell recording, the membrane potential of the cell (V_m), was calculated as $V_m = V_p -$ LJP. All data and IV relationships shown have been corrected for an LJP of 9 mV for low-Cl^-/K^+-aspartate and standard extracellular solution.

Membrane potential and ionic currents were recorded with an amplifier (Axopatch 1D; Axon Instruments, Burlingame, CA). Voltage step commands were generated by a commercial system (Clampex Software, Axon Instruments). Currents were filtered with a four-pole, low-pass Bessel filter (−3 dB at 1 kHz) and digitized at a sampling frequency of 5 kHz by computer (pCLAMP software; Axon Instruments). Current and voltage were displayed on a chart recorder (TA240; Gould Inc., Cleveland, OH) and were stored on computer disc. Values for cell capacitance were obtained from the capacitance com-

pensation circuitry on the amplifier. Measures of series resistance were obtained directly from the amplifier and were always less than 15 MΩ. All experiments were conducted at room temperature (20–24°C).

Western Blot Analysis

Before drug treatments, RPE cells were incubated in low-serum (0.1%) medium for 12 hours to reduce constitutive activation of MAPK. Subsequently, cells were incubated in Hanks' plus 10 μM LPA for 10 minutes at 37°C. In experiments using the MEK inhibitor PD98059, cells were pretreated with 50 μM PD98059 in Hanks' for 25 minutes at 37°C before application of LPA. After washing with Hanks', the cells were centrifuged, and a lysis buffer was added that contained 50 mM Tris-HCl (pH 7.4), 150 mM NaCl, 1 mM EGTA, 1% (octylphenoxy)polyethoxyethanol (IGEPAL CA-630; Sigma Chemical Co.), 0.25% deoxycholic acid, and 10 μL of a protease inhibitor cocktail (Sigma Chemical Co; AEBSF: 100 mM; pepstatin A, 1.5 mM; E-64, 1.4 mM; bestatin, 4 mM; leupeptin, 2.2 mM; and aprotinin, 80 mM). Protein levels were measured by the method of Lowry et al.[32] Treatment buffer (4×) containing 0.125 M Tris, 4% SDS, 20% glycerol, 10% 2-mercaptoethanol, and 1% bromophenol blue was added, and the samples were boiled for 10 minutes. Protein samples (25 μg) and molecular weight markers were separated on a 12% Tris-HCl gel (Ready gel; Bio Rad) at 65 V and transferred overnight onto nitrocellulose (Immobilon P; Millipore, Bedford, MA). The membrane was wetted with methanol and PBS and then incubated for 1 hour at 37°C in PBS containing 5% skim milk, 0.01% Antifoam A (Sigma Chemical Co.), 0.001% thimerosal, and 1% BSA. Blots were incubated overnight at 4°C with a polyclonal extracellular signal-related kinase (ERK)-1 antibody (K-23; Santa Cruz Biotechnology Inc.) diluted 1:500. After extensive washing with PBS-Tween, the blots were reacted with peroxidase-conjugated horse anti-goat antibody (Vector Laboratories, Burlingame, CA) diluted 1:500 for 1 hour at 37°C. After washing, immunostained proteins were visualized using the enhanced chemiluminescence (ECL) Western blot detection technique (Amersham, Arlington Heights, IL).

cAMP Measurements

Levels of cAMP were assayed after prelabelling cells with [^{3}H] adenine, essentially as previously described.[33,34] Cells were washed with serum-free DMEM and then incubated for 60 minutes at 37°C with DMEM containing 2 μCi [^{3}H] adenine per 35-mm tissue culture dish to label cellular ATP pools. This medium was removed, and cells were rinsed with DMEM and then incubated in test solutions for 2 minutes at 37°C. Test medium was aspirated, the reaction was stopped, and cellular nucleotides were extracted with 1 mL 5% trichloroacetic acid. [^{3}H]ATP and [^{3}H]cAMP in the extracts were then separated by sequential chromatography over Dowex (Dow Chemicals, Midland, MI), and alumina columns and quantified with a liquid scintillation counter. cAMP accumulation is expressed as the percentage conversion of [^{3}H]ATP to [^{3}H]cAMP. Each experiment was repeated a minimum of three times on cells from at least three donor eyes.

IP Measurements

IP formation was measured using a [^{3}H]inositol labeling procedure, described in previous studies.[34–36] Cells were washed with serum-free DMEM and incubated at 37°C overnight in inositol-free DMEM containing 2 μCi [^{3}H]inositol per 35-mm culture dish. Cells were washed, incubated in the test solution plus 10 mM LiCl for 20 minutes, washed again, and the reaction was stopped with addition of 500 μL methanol. The cells were scraped from the dish, placed in glass tubes, and extracted with chloroform, water, and additional methanol (final ratio of 1:0.9:1 vol/vol/vol). The aqueous phase was applied to Dowex 1-X8 (formate form) columns. Total IP were collected as a single fraction by elution with 8 mL of 1 M ammonium formate-0.1 M formic acid and quantified with a liquid scintillation counter. IP formation is expressed as the percentage conversion of [^{3}H]inositol phospholipids to [^{3}H] inositol phosphates. Each experiment was repeated a minimum of three times on cells from at least three donor eyes.

Calcium Measurements

Intracellular Ca^{2+} changes were monitored using the ratiometric dye fura-2. RPE cells were incubated for 45 minutes in fura-2/AM (10 μM; Molecular Probes, Eugene, OR) plus nonionic detergent (10 μM; Pluronic F127; Boitium, Hayward, CA). After loading, cells were rinsed (1 mL/min) for 30 minutes by perfusion with an oxygenated solution containing (in mM): NaCl, 140; KCl, 5; $CaCl_2$, 2; $MgCl_2$, 1; HEPES, 10; glucose, 10 (pH 7.4). Test solutions were applied by bath perfusion, and experiments were performed at room temperature. Ca-free medium contained (in mM): NaCl, 140; KCl, 5; $MgCl_2$, 1; HEPES, 10; glucose, 10; EGTA, 10 (pH 7.8). Cells were viewed through a 60× water-immersion objective (1.0 numeric aperture; Nikon) on an upright, fixed-stage microscope (E600FN; Nikon). Fluorescence was stimulated with a 150-W Xenon lamp attached to the microscope's epifluorescence port by liquid light guide (Sutter Instruments), and excitation wavelengths (340 or 380 nm) were changed with a filter wheel (Lambda 10-2; Sutter Instruments). Fluorescence changes were monitored with a cooled charge-coupled device (CCD) camera (SensiCam; Cooke Corp., La Jolla, CA) using image-analysis software (Imaging Workbench; Axon Instruments). Images were typically acquired every 5 to 10 seconds using 1 × 1 or 2 × 2 binning with 0.5- to 1-second acquisition times. Ca^{2+} responses were measured as the highest peak Ca^{2+} level obtained 50 to 70 seconds after beginning perfusion of LPA or ATP (to allow for delay in the perfusion lines) and compared with the control level measured immediately before drug application.

Determination of intracellular Ca^{2+} concentrations was performed using the ratiometric method of Grynkiewicz et al.[37] Instrumental changes were monitored with periodic determinations of K_{eff} (the effective dissociation constant of fura-2), R_{max} (the limiting ratio at zero calcium), and R_{min} (the limiting ratio at saturating calcium), by using micropipettes filled with 10 μM fura-2 pentapotassium salt (Molecular Probes) in solutions containing various concentrations of Ca^{2+} ranging from Ca^{2+}-free to 1.8 mM Ca^{2+}.

RT-PCR and RNase Protection Assays

Total RNA was extracted from RPE cells by using an extraction reagent (TRIzol; Life Technologies) according to the manufacturer's instructions. RT-PCR was performed with primers specific for the human Edg2, -4, and -7 receptors, based on the GenBank sequence accession numbers U80811, AF011466, and AF186380, respectively (GenBank is provided in the public domain by the National Center for Biotechnology Information, Bethesda, MD, and is available at http://www.ncbi.nlm.nih.gov/Genbank). Oligonucleotide primers used for Edg2 were forward 5′-ccatctctacttccatccc and reverse 5′-caatgaccaccactaccc. Primers used for Edg4 were forward 5′-ctggtcaagactgttgtcatc and reverse 5′-atctcagcatctcggcaag. Primers used for Edg7 were forward 5′-tgactgcttccctcaccaac and either reverse 5′-tccagcataccacaaacgcc (for RT-PCR experiments shown) or reverse 5′-ccacttgtatgcggagacaag (for RPA experiments shown). The RT-PCR studies shown in Figure 12 were performed using a reverse primer in the coding region for transmembrane domain VI. The resultant amplicon contained a consensus splice site[2] and occasionally yielded a doublet product when used as an RNase protection assay (RPA) probe. To exclude the potential splice site, a smaller probe was generated with the second reverse primer listed, which is in the region coding for the third intracellular loop of the Edg7 receptor. This probe was used for the RPA shown in Figure 13. RT-PCR was performed using a commercial system (Robocycler Gradient 40; Stratagene, La Jolla, CA). For reverse transcription, the samples were held at room temperature for 15 minutes and then incubated at 37°C for 60 minutes and then at 98°C for 5 minutes. The PCR included an initial denaturation at 95°C for 5 minutes followed by 35 cycles, each with 1 minute of denaturation at 95°C, 1 minute of annealing at 55°C, and 1 minute of extension at 72°C. The final extension was for 5 minutes at 72°C.

Riboprobes for RNase protection assays were generated by cloning RT-PCR products from reactions with human airway smooth muscle cell RNA into the TOPO II vector using a cloning kit (TOPO-TA; Invitrogen, San Diego, CA). Vectors were sequenced and then linear-

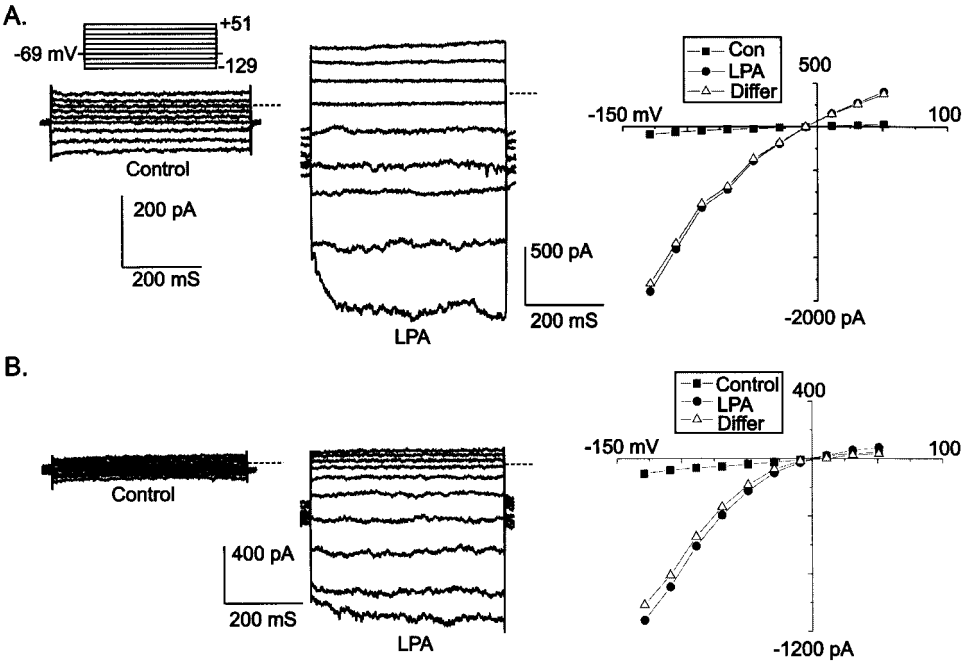

FIGURE 1. LPA activated an inwardly rectifying current in cultured rat RPE cells. (**A**) Whole-cell current recording from a representative rat RPE cell in the absence (Control, *left*) or presence (LPA, *middle*) of 100 μM LPA. Currents were recorded in standard low-Cl^-, 100-mM K^+-aspartate intracellular, and standard 5-mM K^+ extracellular solutions. *Right*: I-V plot for the control, LPA, and LPA-difference (LPA-activated current − control current) currents. (**B**) Whole-cell currents recorded in low-Cl^-, 100-mM Cs^+-aspartate intracellular, and K^+-free extracellular solution in the absence (Control, *left*) and presence (LPA, *middle*) of 100 μM LPA. *Right*: I-V plot for the control, LPA, and LPA-difference currents in the absence of K^+.

ized to be used as templates for in vitro transcription with a kit (MaxiScript; Ambion, Austin, TX). Biotinylated cytosine triphosphate (CTP; Life Technologies) was included in the transcription reaction at a 1:1 ratio with nonbiotinylated CTP to generate biotinylated probe. RNase protection assays were then performed with a kit (RPA III; Ambion) according to the manufacturer's instructions. Briefly, biotinylated anti-sense probe RNA and RPE cell total RNA were hybridized overnight at 42°C. Single-stranded RNA was digested for 30 minutes at 37°C with a 1:100 dilution of RNase A/T1 mixture. Double-stranded RNA was then precipitated and separated by denaturing polyacrylamide gel electrophoresis of 5% polyacrylamide gels. Samples were then transferred to membranes (BrightStar-Plus; Ambion), and probe was detected using a kit (BrightStar BioDetect; Ambion). Blots were exposed to film (Biomax; Eastman Kodak, Rochester, NY) and analyzed with a scanning laser densitometer (Molecular Dynamics, Sunnyvale, CA).

Chemicals

Unless otherwise noted, all culture reagents were from Life Technologies, and chemicals were obtained from RBI/Sigma Chemical Co.

Statistical Analysis

Data are presented as mean ± SEM and analyzed by use of Student's *t*-test, unless otherwise noted. $P < 0.05$ was accepted as significant.

RESULTS

LPA application to cultured human RPE cells evokes a nonselective cation current.[14] We tested the actions of LPA on rat RPE cells. Figure 1A shows whole-cell currents recorded from a cultured rat RPE cell in standard external solution with K-aspartate in the pipette. The cells were held at −69 mV and stepped to potentials negative and positive to the holding potential. In the absence of LPA, inward and outward currents were apparent (Fig. 1A, left). These currents have been described previously and are K^+ currents.[25] A 30-second puffer application of LPA (100 μM) evoked a large increase in inward current, with a smaller increase in outward current (Fig 1A, middle). The IV profile for the currents recorded with and without LPA, as well as the LPA-activated difference current, obtained by subtracting current measured in the absence of LPA from current in the presence of LPA, are shown in Figure 1A (right). The current evoked by LPA was inwardly rectifying and reverses at −10 mV (Fig. 1A, right). To further confirm LPA-activation of a nonselective cation current, whole-cell currents were recorded in solutions designed to minimize activation of both inward and outward K^+ currents. Figure 1B shows whole-cell currents recorded from a representative cell in K^+-free external solution with Cs-aspartate in the pipette and in the absence of LPA (Fig. 1B, left). As before, in the presence of LPA, an increase in inward current was apparent (Fig 1B, middle). The IV relationships in whole-cell currents in the absence and presence of LPA, as well as the LPA-difference current, are shown in Figure 1B (right). With K^+ currents blocked, LPA activated an inwardly rectifying cation current that reverses close to 0 mV (±5 mV).

Figure 2 shows the mean I-V relationship recorded in 10 cells, in standard 5 mM K^+ external solution with K^+-aspartate internal solution, in the presence and absence of LPA (100 μM). Application of LPA produced an increase in inward current in all cells tested, with a positive shift in the zero current potential and an increase in conductance at negative potentials (from 91 ± 25 to 278 ± 73 pS/pF at -129 mV and from 18 ± 7.5 to 114 ± 23 pS/pF at -69 mV, respectively, $n = 10$). Figure 2B shows mean current amplitudes for the LPA-activated difference current at various potentials. Consistent with activation of an inward cation current, the LPA-activated current is inward at the K^+ equilibrium potential of −89 mV and at the Cl^- equilibrium potential of −49 mV, but is outward at +31 mV (Fig. 2B; $n = 10$). Taken together, these results suggest that, as in human RPE cells, LPA primarily activates a nonselective cation current in cultured rat RPE cells. Furthermore, as in human RPE cells,[14] LPA occasionally activates both inward and outward K^+ currents in rat RPE cells (<20% of cells). However, mean outward current recorded at positive potentials in the presence of LPA was not significantly different from the control (Fig. 2B).

Activation of G_i-protein–coupled pathways has been associated with LPA receptor activation,[1,2] and a G_i-coupled MAPK pathway has been shown to modulate nonspecific cation cur-

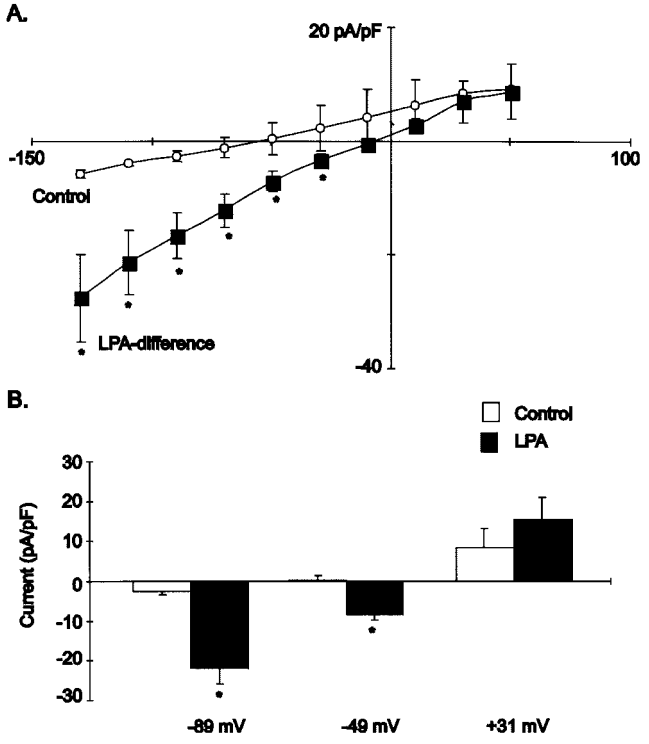

FIGURE 2. Inward current activated by LPA was a nonselective cation current. (**A**) I-V plot for mean ± SEM current amplitude measured in 10 representative rat RPE cells before (○) and after (■) a 30-second puffer application of 100 μM LPA. Whole-cell currents were normalized for cell capacitance. (**B**) Mean ± SEM current amplitude measured at −89 mV (K^+ equilibrium potential), −49 mV (Cl^- equilibrium potential), and +31 mV in the same 10 cells before (□) and after (■) a 30-second application of 100 μM LPA. $^*P < 0.05$ relative to control.

rents in rat RPE cells.[25,26] We examined whether LPA-activation of cation current in RPE cells involved G_i-coupled signaling pathways by loading cells with antibodies to α-subunits of the G protein, $G_{i/o/t/z}$, and measuring the LPA-difference current (Fig. 3A). Loading cells with anti-$G_{\alpha i/o/t/z}$ blocked LPA stimulation of cation currents in rat RPE cells. This result is consistent with the finding in human RPE cells that PTx-pretreatment inhibits LPA-evoked cation currents.[14]

We also tested the effects of a protein tyrosine kinase (PTK) inhibitor, genistein, and the MEK inhibitor PD98059 on LPA-evoked cation currents. Genistein (100 μM) significantly reduced LPA-evoked inward currents ($P < 0.05$, Fig. 3A), whereas its less active analogue, daidzein (100 μM), did not significantly inhibit LPA-evoked cation currents (data not shown). LPA activation of cation currents was also blocked by PD98059 (50 μM, $P < 0.05$, Fig. 3A), suggesting that the LPA-evoked cation current may be modulated by a PTK- and MAPK-coupled signaling pathway.

We further confirmed that LPA activated MAPK in RPE cells using Western blot analysis with antibodies to the MAPK kinase, ERK-1 (Fig. 3B). In control (plus DMSO) and LPA-stimulated conditions, two distinct bands were observed: a lower 44-kDa band reflecting unstimulated ERK-1 and a second higher band representing the shift in mobility associated with phosphorylated (activated) ERK-1, which runs at an increased apparent molecular weight.[38] In control cells, both bands were present and appeared roughly equivalent (Fig. 3B, lane 1). The appearance of the upper phosphorylated ERK-1 band in the DMSO control group may reflect some activation of ERK-1 related to cellular stress on removal of attached cells from the culture flasks, media changes or inclusion of DMSO.[39] However, levels of the phosphorylated protein relative to unstimulated ERK-1 were enhanced above DMSO control levels by incubation in LPA (Fig. 3B, second lane). The LPA-induced increase in phosphorylated ERK-1 was completely blocked by the MEK inhibitor PD98059, which reduced phosphorylated ERK-1 below levels apparent in control groups but did not block the unstimulated protein (Fig. 3B, third lane). Data in Figure 3C are taken from densitometry measurements of the upper phosphorylated ERK-1 band shown in Figure 3B and indicate that LPA produces a more than 50% increase in activation of ERK-1, which is blocked by PD98059. Taken together, these data suggest that activation of LPA receptors stimulates PTx-sensitive $G_{i/o/t/z}$ proteins, with increases in tyrosine kinase and MAPK activity and activation of a nonselective cation current.

Activation of $G_{\alpha i}$ typically produces inhibition of cAMP accumulation. Effects of LPA on forskolin (50 μM)-stimulated cAMP accumulation were therefore tested in cultured human RPE cells with a [^{3}H]adenine preloading procedure. Figure 4

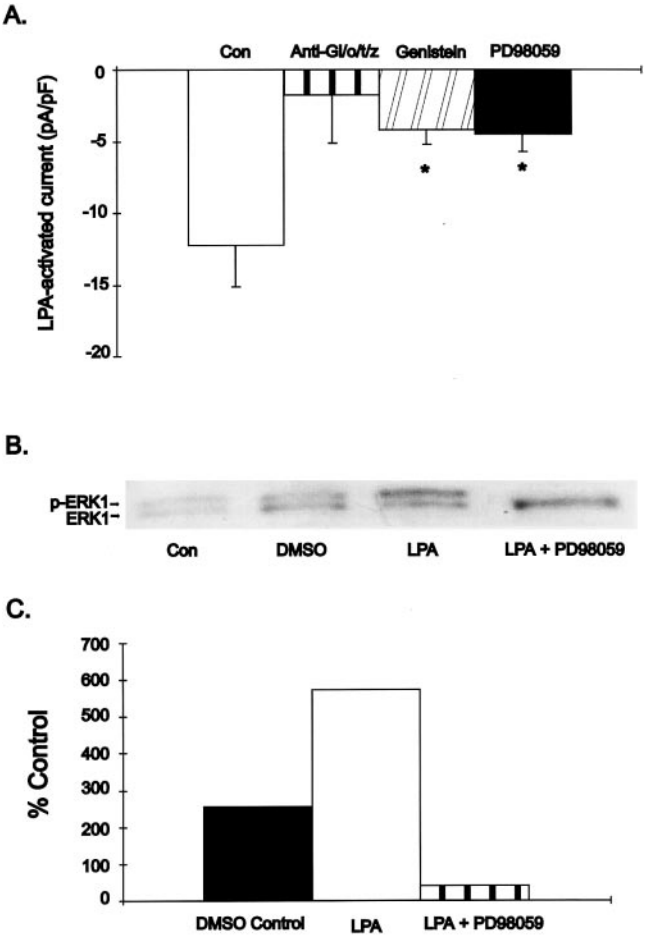

FIGURE 3. G proteins and an MAPK pathway were involved in the LPA-activated inwardly rectifying cation current in a rat RPE cell. (**A**) Mean current amplitude ± SEM for the LPA-activated difference current measured at −69 mV in the absence (control; $n = 16$) or presence of 50 μM PD98059 ($n = 7$), anti-$G_{\alpha i/o/t/z}$ ($n = 4$), or 100 μM genistein ($n = 4$). All data were normalized for cell capacitance. $^*P < 0.05$. (**B**) Western blot analysis showing phosphorylated (*top band*) and unphosphorylated (44 kDa, *bottom band*) ERK-1 in control cells in the presence of DMSO (0.1%) minus drug, in LPA (10 μM, +0.1% DMSO) alone, and in LPA after a 25-minute preincubation with the MEK inhibitor PD98059 (50 μM). (**C**) Change in phosphorylated ERK-1 relative to total protein (normalized to control) in DMSO control, LPA, and LPA+PD98059.

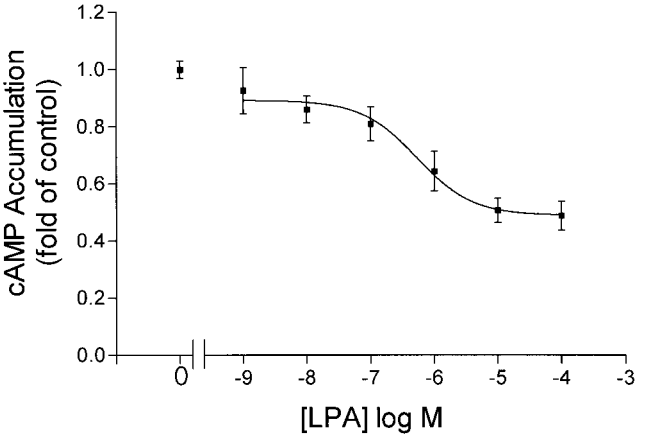

FIGURE 4. LPA inhibited forskolin-stimulated (50 μM) cAMP accumulation in a dose-dependent manner in cultured human RPE cells. Dose–response data were fit with a sigmoidal curve: $r/r_{max} = [1 + (c/IC_{50})]^{-1}$ where r is the test cAMP level/control cAMP level, r_{max} is the maximum fractional response, c is the test concentration, and IC_{50} is the midpoint of the sigmoid. Best fit $IC_{50} = 5.4 \times 10^{-7}$ M (log $IC_{50} = -6.3 \pm 0.32$). Data are from 15 trials in five experiments with cells from five donor eyes. Inhibition of cAMP accumulation by LPA is significant at $P < 0.0001$ (one-way ANOVA).

shows that LPA produced a dose-dependent inhibition of forskolin-stimulated cAMP accumulation with a 50% inhibitory concentration (IC_{50}) of 0.54 μM. LPA (100 μM) also significantly inhibited the production of cAMP evoked by the β-adrenergic agonist, isoproterenol (10 μM, data not shown).

Consistent with the possibility that inhibition of cAMP accumulation by LPA (10 μM) is partly mediated by PTx-sensitive G proteins, 12-hour pretreatment with PTx (100 ng/mL) blocked effects of LPA in cultured human RPE cells derived from one donor eye (Fig. 5A). However, PTx-pretreatment did not significantly reduce LPA effects in cells derived from two other donor eyes (Figs. 5B, 5C), suggesting that either there are multiple pathways by which LPA can inhibit cAMP accumulation or that there may be differences in PTx uptake and sensitivity of G protein block in cells from different donor eyes. We tested the possibility that cAMP accumulation might be inhibited by stimulation of phosphodiesterase activity. Although the phosphodiesterase blocker IBMX (100 μM) enhanced forskolin-stimulated cAMP accumulation, it did not prevent the inhibition of cAMP accumulation by LPA (10 μM, data not shown). This was true even in cells from one of the donor eyes, in which LPA responses were not blocked by PTx pretreatment. Although we cannot rule out a small contribution of phosphodiesterase activity, this result suggests that it is not a major contributor to LPA-induced inhibition of cAMP accumulation.

LPA receptors can stimulate IP_3 production through both G_i and G_q-mediated mechanisms.[1,2] We therefore tested the effects of LPA on IP formation. As a positive control, we also tested effects of ATP, because human RPE cells appear to possess P2Y2 nucleotide receptors[24] and activation of P2Y2 receptors by ATP stimulates phospholipase C and thus production of IP_3.[40,41] ATP (100 μM) stimulated a 2.6 $\pm$ 0.66-fold increase in formation of IP, whereas LPA (10–100 μM) had no significant effect (Fig. 6).

Despite the absence of IP production, we found that LPA stimulated Ca^{2+} increases in human RPE cells loaded with fura-2 (Fig. 7). LPA evoked Ca^{2+} increases in 24 of 48 cells (20–100 μM) derived from five separate donor eyes. Consistent with previous studies showing that activation of purinergic receptors by ATP induces release of Ca^{2+} from intracellular stores in RPE cells,[24,42–44] ATP (100 μM) evoked Ca^{2+} responses in 28 of 45 cells tested. The presence of LPA-evoked Ca^{2+} increases was not correlated with the presence of ATP-evoked Ca^{2+} increases. Ca^{2+} responses evoked by LPA exhib-

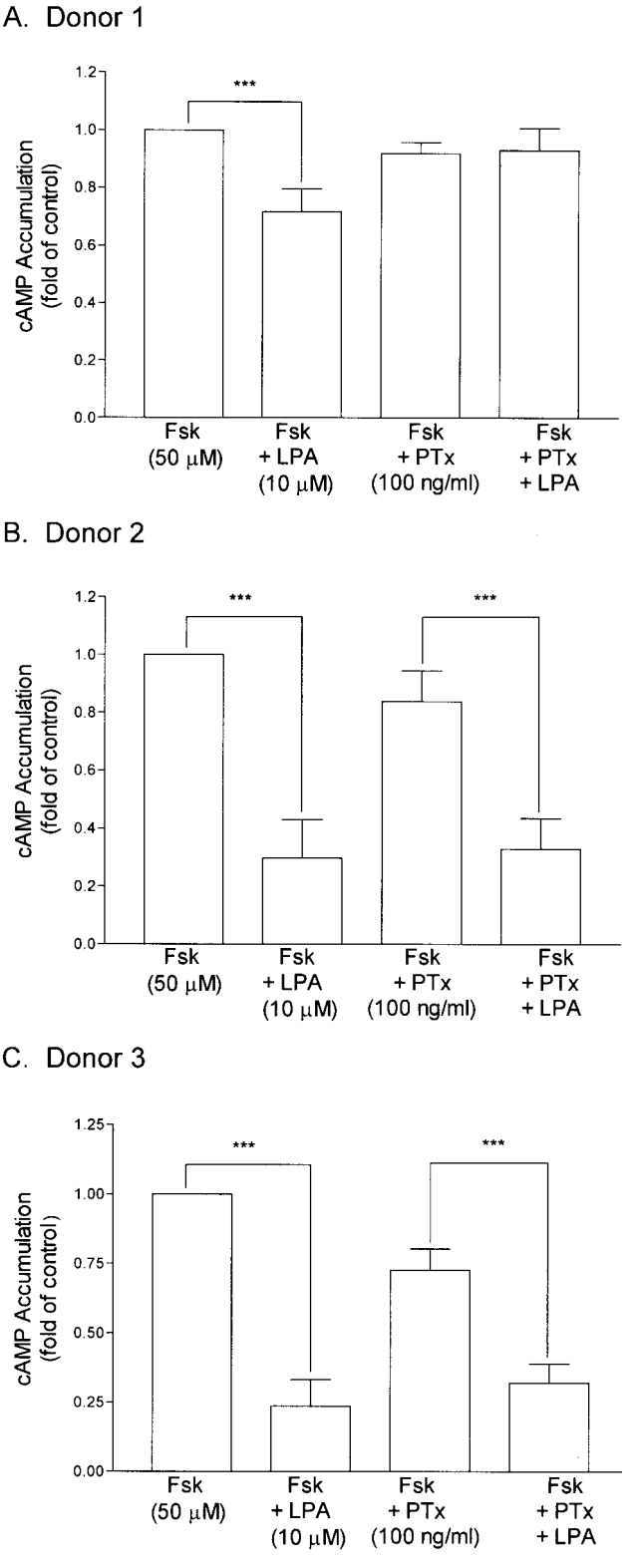

FIGURE 5. PTx pretreatment (100 ng/mL) blocked inhibition of forskolin (Fsk)-stimulated cAMP accumulation by LPA (10 μM) in cultured human RPE cells of donor 1 (**A**), but not in those of donors 2 (**B**) and 3 (**C**). ***$P < 0.001$. Donor 1: 26 trials in six experiments; donor 2: 9 trials in three experiments; donor 3: 12 trials in three experiments.

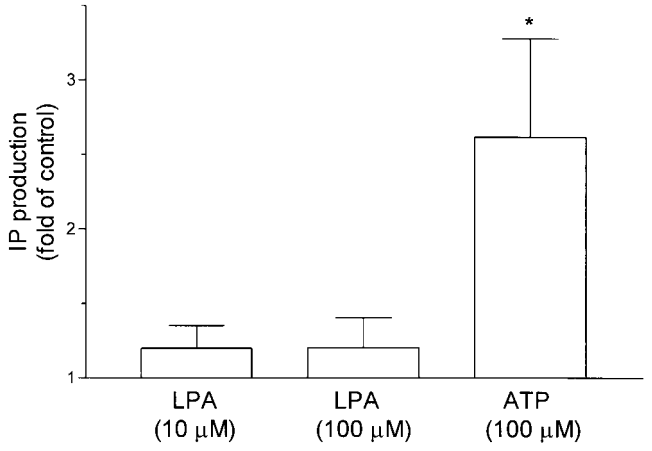

FIGURE 6. ATP (100 μM), but not LPA (10–100 μM), stimulated a significant increase in IP formation in cultured human RPE cells. $^*P < 0.05$. In all three conditions, 12 trials in four experiments were performed in cells from three donor eyes.

ited much greater rundown, with repeated applications than did responses evoked by ATP. Repeated applications of ATP evoked similar Ca^{2+} responses in 9 of 11 cells tested (e.g., Fig. 7B). In contrast, Ca^{2+} increases evoked by LPA were greatly diminished or absent after prior application of LPA (e.g., Fig. 7C). For this reason, we could perform only one experiment with LPA per cell, making it necessary to compare treatment and control conditions using different samples of cells. Furthermore, because of the marked response rundown, we could not reliably determine which cells possessed the capacity to respond to LPA by using control applications of LPA. Therefore, all tested cells and their matched control were included in statistical comparisons regardless of whether a detectable Ca^{2+} increase was observed. To avoid potential artifacts that might be introduced by differences in the frequency of LPA-responsive cells among RPE cells derived from different donor eyes, similar proportions of cells from the same lineage were used in both control and test conditions for each experiment.

Cells derived from one donor (donor 5) consistently exhibited increases in $[Ca^{2+}]_i$ when LPA was applied at concentrations of 1 μM or more. Other than the higher frequency of responses, the nature of the Ca^{2+} responses evoked by LPA in cells of the eye of donor 5 appeared fundamentally similar to the responses from cells derived from other donors. Similar to cells from other donor eyes (compare with data in Figs. 9 and 10), Ca^{2+} responses in cells of donor 5 to LPA were significantly reduced in Ca^{2+}-free medium ($P < 0.0001$) and by preloading the cells with antibodies to $G_{\alpha i/o/t/z}$ ($P < 0.0001$), but not by U73122 (20 μM, $P = 0.33$). We used cells from donor 5 to obtain concentration–response data for LPA-evoked Ca^{2+} increases. As illustrated in Figure 8, application of LPA produced a concentration-dependent increase in Ca^{2+} responses with an EC_{50} of 0.36 μM.

The phospholipase C blocker, U73122, did not significantly inhibit increases in $[Ca^{2+}]_i$ evoked by LPA (e.g., Fig. 9; 100 μM, $P = 0.32$, $df = 65$, cells derived from three donors; 1 μM, $P = 0.33$, $df = 17$, cells from donor 5). The ability of U73122 (20 μM) to inhibit phospholipase C in these cells is supported by its strong inhibition of ATP-evoked Ca^{2+} increases (Fig. 9) in all 13 cells that responded to ATP in control medium. When combined with the results showing that LPA did not stimulate IP production, these results indicate that LPA-evoked Ca^{2+} responses do not arise from stimulation of IP_3 production.

We tested whether the Ca^{2+} response evoked by LPA required the presence of extracellular Ca^{2+}. As shown in Figure 10A, application of LPA in the presence of Ca^{2+}-free medium (10 mM EGTA) evoked significantly smaller Ca^{2+} responses than LPA applied in control medium, suggesting a dependence on extracellular Ca^{2+}. However, LPA-evoked Ca^{2+} responses were not completely abolished in Ca^{2+}-free medium, indicating that a component of the response involves release of Ca^{2+} from intracellular stores. Furthermore, the diminution of LPA-evoked Ca^{2+} increases produced by application of Ca^{2+}-free medium appeared to be at least partly a secondary consequence of depletion of intracellular stores, because ATP-evoked Ca^{2+} responses were also diminished in Ca^{2+}-free

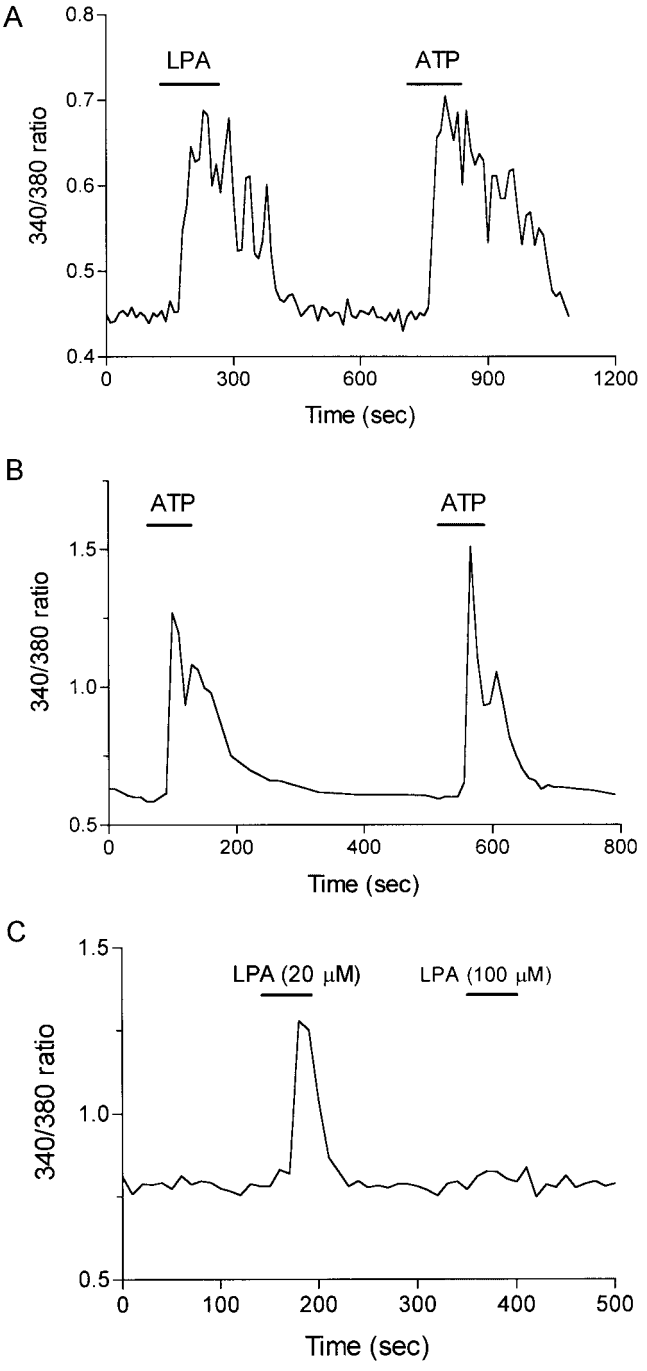

FIGURE 7. (**A**) Both LPA (100 μM) and ATP (100 μM) evoked increases in intracellular Ca^{2+} measured with fura-2 in individual cultured human RPE cells. (**B**) Repeated applications of ATP evoked similar increases in $[Ca^{2+}]_i$. (**C**) LPA-evoked increases in $[Ca^{2+}]_i$ were greatly diminished with repeated application of LPA.

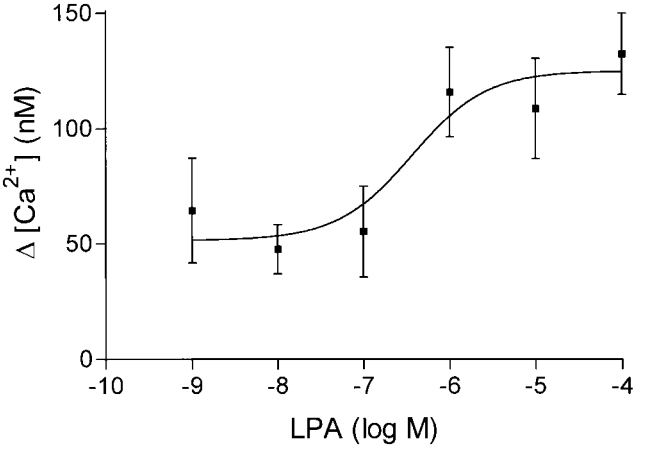

FIGURE 8. LPA evoked a concentration-dependent increase in $[Ca^{2+}]_i$ in cells of donor 5. Concentration–response data were fit with a sigmoidal curve: $r/r_{max} = [c/(c + EC_{50})]$ where r is the change in $[Ca^{2+}]_i$, r_{max} is the maximum change in $[Ca^{2+}]_i$, c is LPA concentration, and EC_{50} is the midpoint of the sigmoid. Best fit $EC_{50} = 3.6 \times 10^{-7}$ M (log $EC_{50} = -6.44 \pm 0.57$). Concentration-dependent increase in $[Ca^{2+}]_i$ evoked by LPA is significant at $P = 0.0076$ (one-way ANOVA). 10^{-9} M, $n = 9$; 10^{-8} M, $n = 13$; 10^{-7} M, $n = 7$; 10^{-6} M, $n = 10$; 10^{-5} M, $n = 10$; 10^{-4} M, $n = 10$.-

medium (Fig. 10A). As a further test of whether release of Ca^{2+} from intracellular stores contributes to LPA-evoked Ca^{2+} increases, we tested the impact of depleting Ca^{2+} stores with thapsigargin (1 μM). Both LPA- and ATP-evoked Ca^{2+} increases were significantly reduced by prior application of thapsigargin (Fig. 10B). The results of Figure 6 and 9 suggest that LPA-evoked Ca^{2+} increases do not involve IP_3. We tested involvement of another major Ca^{2+}-release pathway by using ryanodine (20 μM). To isolate intracellular release mechanisms from influx pathways, we applied ryanodine in Ca^{2+}-free conditions. As shown in Figure 10C, ryanodine did not significantly alter the amplitude of Ca^{2+} responses under these conditions, suggesting that ryanodine receptors are unlikely to be involved in the LPA-evoked release of Ca^{2+} from intracellular stores.

A contribution from Ca^{2+} influx to LPA-evoked Ca^{2+} increases is suggested by the finding that Cd^{2+} (3 mM), which inhibits LPA-stimulated cation channels,[14] inhibited the amplitude of Ca^{2+} increases evoked by LPA (10 μM) in cells of donor 5 ($P = 0.018$; $df = 25$). (Consistent with the results indicating a role for release from intracellular stores, LPA nonetheless stimulated Ca^{2+} increases in all 14 cells tested in the presence of Cd^{2+}.) It is unlikely that Ca^{2+} influx was due to stimulation of cAMP-gated cation channels, because LPA inhibited, rather than stimulated, cAMP production. It is also unlikely that cGMP-gated cation channels were responsible for Ca^{2+} increases in human RPE cells, because 0.5 mM 8-Br-cGMP failed to produce a detectable Ca^{2+} response in 29 cells tested (data not shown). Cultured human RPE cells have been shown to express high-voltage–activated, L-type Ca^{2+} channels.[14,45,46] However, nisoldipine (5 μM) did not significantly inhibit Ca^{2+} increases evoked by LPA in donor 5 (10 μM; $P = 0.813$, $df = 19$).

We tested whether Ca^{2+} responses in RPE cells involve activation of PTx-sensitive G proteins and the MAP kinase pathway. First, we tested the effects of LPA on human RPE cells loaded with antibodies to $G_{\alpha i/o/t/z}$. Loading with the antibody significantly reduced the amplitude of LPA-evoked responses in cells derived from five different donor eyes (Fig. 11A). We also tested the ability of PD98059 and genistein to inhibit Ca^{2+} responses. The Ca^{2+} responses evoked by LPA (1 μM) in cells of donor 5 were significantly inhibited by PD98059 (50 μM). Responses were not significantly inhibited by genistein (100 μM; $P = 0.12$) or its less active analogue, daidzein (100 μM; $P = 0.21$).

We used RT-PCR to test for the presence of RNA for the three LPA receptor subtypes Edg2, -4, and -7. As shown in Figure 12, PCR performed after reverse transcriptase application (RT+) yielded bands of the size predicted from the primers used for the three receptor subtypes: Edg 2 at 498 bp, Edg4 at 191 bp, and Edg7 at 419 bp, indicating that at least low levels of RNA for all three receptor subtypes are present in RPE cells.

To assess relative RNA levels for each receptor subtype we used an RPA to examine LPA receptor RNA. As shown in Figure 13, using 10 μg of RNA from human RPE cells, a 498-bp band representing Edg-2 was clearly visible, whereas bands for Edg4 and Edg7 were not detected. As a positive control, we also performed RPAs on RNA from human airway smooth muscle cells (Fig. 13B). In these cells, bands for all three receptors were observed. These results suggest that, although RNAs for all three LPA receptor subtypes were detected in RPE cells by RT-PCR, RNA for Edg2 appeared to be particularly abundant.

DISCUSSION

The results of this and previous studies[14,15] indicate that LPA engages multiple signal-transduction pathways within RPE cells. In other cell types, LPA receptors have been shown to activate at least three classes of G proteins: G_i, leading to inhibition of cAMP production, stimulation of MAPK, and, in some cells, stimulation of phospholipase C; G_q, leading to stimulation of phospholipase C; and $G_{12/13}$, leading to stimulation of the small GTPase Rho.[1] The LPA receptor subtype Edg2 appears to couple to G_i and $G_{12/13}$, whereas Edg4 and -7 receptors couple predominately to G_q.[1,23] RPE cells exhibited strong expression of Edg2 (Fig. 13), consistent with the results of signal transduction experiments that suggest that LPA receptors in RPE cells activate G_i (leading to inhibition of adenylyl cyclase and activation of MAPK) and possibly $G_{12/13}$ (leading to activation of Rho), but not G_q. The G_i-coupled signaling pathways suggested by the present results are illustrated schematically in Figure 14. The evidence for these conclusions is considered in the following discussion.

Activation of G_i by LPA receptors is supported by the findings that RPE cell proliferation,[15] inhibition of cAMP accumulation in some cells (Fig. 5), and activation of the cation current[14] are all blocked by PTx. An antibody to the PTx-sensitive G proteins, $G_{\alpha i/o/t/z}$, also blocked LPA-evoked cation

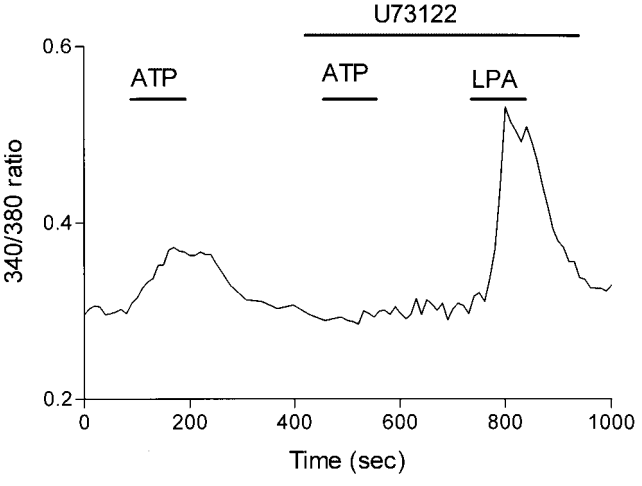

FIGURE 9. Phospholipase C inhibitor, U73122 (20 μM), blocked responses to ATP (100 μM) but not to LPA (100 μM).

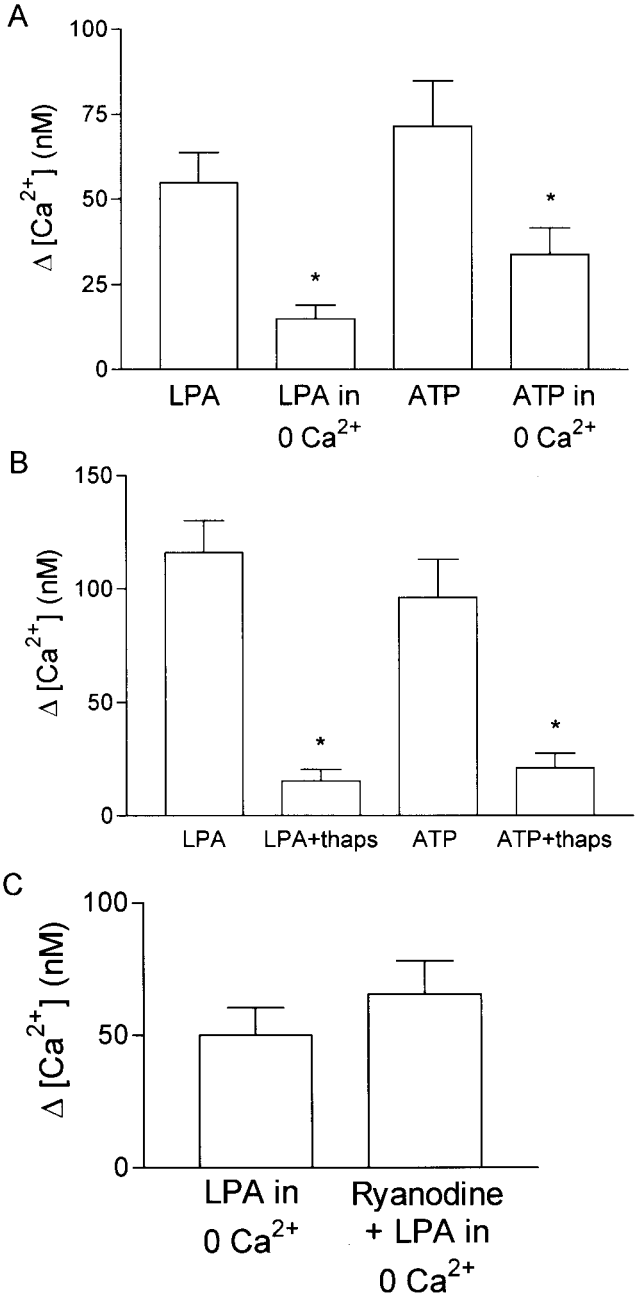

FIGURE 10. (**A**) Increases in $[Ca^{2+}]_i$ evoked by LPA (100 μM) and ATP (100 μM) were inhibited by 3 minutes or longer perfusion with Ca^{2+}-free medium containing 10 mM EGTA (LPA: $P < 0.0001$, $df = 122$, tested in cells from four donor eyes; ATP: $P = 0.023$, $df = 90$; tested in cells from three donor eyes). The smaller amplitude of control Ca^{2+} increases in (**A**) compared with Figure 10 or (**B**) reflects differences among different samples of cells. (**B**) Ca^{2+} increases evoked by LPA (100 μM) and ATP (100 μM) were inhibited by pretreatment for 3 minutes or longer with 1 μM thapsigargin (thaps; LPA: $P < 0.0001$, $df = 81$; ATP: $P = 0.0089$, $df = 63$; tested in cells from three donor eyes). (**C**) Ryanodine (20 μM) applied in Ca^{2+}-free medium did not significantly alter Ca^{2+} responses evoked by LPA (1 μM) in cells derived from donor 5 ($P = 0.36$; $df = 24$).

currents (Fig. 3) and LPA-evoked increases in intracellular Ca^{2+} (Fig. 11). The present results show that activation of LPA receptors in RPE cells stimulated phosphorylation of ERK-1 and that this stimulation was reduced by inhibition of MEK (Fig. 3). Consistent with the hypothesis that cation currents activated by LPA are regulated by MAPK activation, inhibition of MAPK by the MEK inhibitor PD98059 or inhibition of upstream activators, such as tyrosine kinase, blocked LPA-evoked cation current activity (Fig. 3). PD98059 also blocked LPA-evoked Ca^{2+} responses (Fig. 11), suggesting that MAPK activation is also involved in these responses.

Stimulation of MAPK has been shown to regulate a cation current in RPE cells.[26] However, the GTPγS-induced nonspecific cation current in rat RPE cells[25,26] exhibits less rectification than the LPA-induced cation current in rat RPE cells, and in this respect is more similar to LPA-activated cation currents in human RPE cells[14] and in bovine and human Müller cells.[13] Some characteristics of the LPA-evoked cation current in rat RPE cells (inward rectification, nonselective for cations) also qualitatively resembled the cyclic guanosine monophosphate (cGMP)–activated cation current previously described in rat RPE cells,[26] although a cGMP-activated cation current was absent in cultured human RPE cells (Thoreson WB, unpublished observations, 1996). It is possible that LPA receptor stimulation of multiple signaling pathways involving MAPK activation and increases in intracellular Ca^{2+} may directly or indirectly modulate the activity of one or several different cation channels in RPE cells that can contribute to whole-cell current.

LPA-evoked Ca^{2+} responses were reduced in Ca^{2+}-free medium or by bath application of Cd^{2+} suggesting that Ca^{2+} influx contributes to the intracellular Ca^{2+} increase. As considered in the Results section, LPA-evoked Ca^{2+} influx in human RPE cells is unlikely to involve cyclic nucleotide-gated

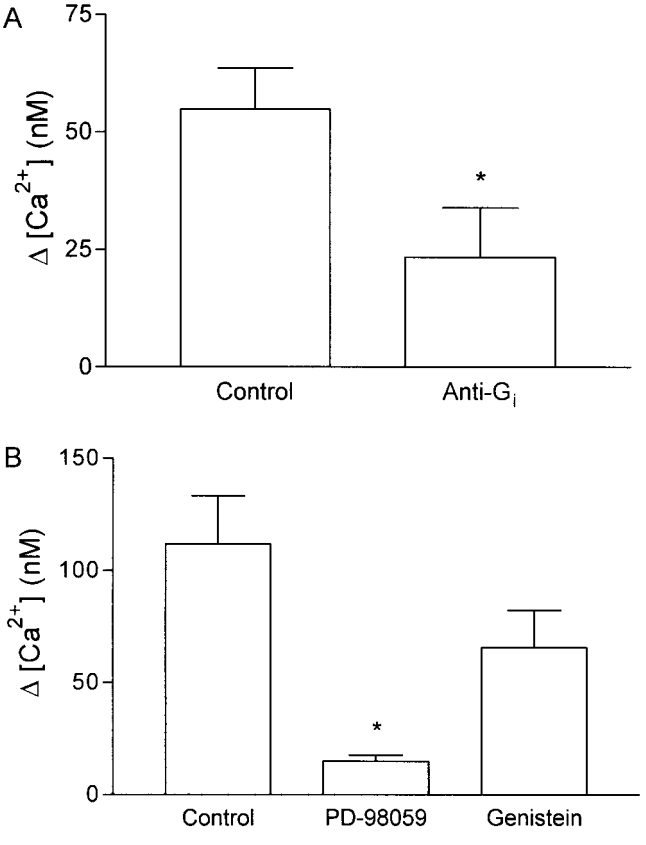

FIGURE 11. (**A**) Increases in $[Ca^{2+}]_i$ evoked by LPA (100 μM) were significantly inhibited in RPE cells which had been loaded with anti-$G_{\alpha i/o/t/z}$ ($P = 0.023$, $df = 89$, tested on cells of five donor eyes). (**B**) PD98059 (50 μM), but not genistein (100 μM), significantly inhibited LPA-evoked increases in $[Ca^{2+}]_i$ evoked by LPA (1 μM) in cells from donor 5 (PD98059: $P = 0.0002$, $df = 19$; genistein: $P = 0.12$, $df = 16$).

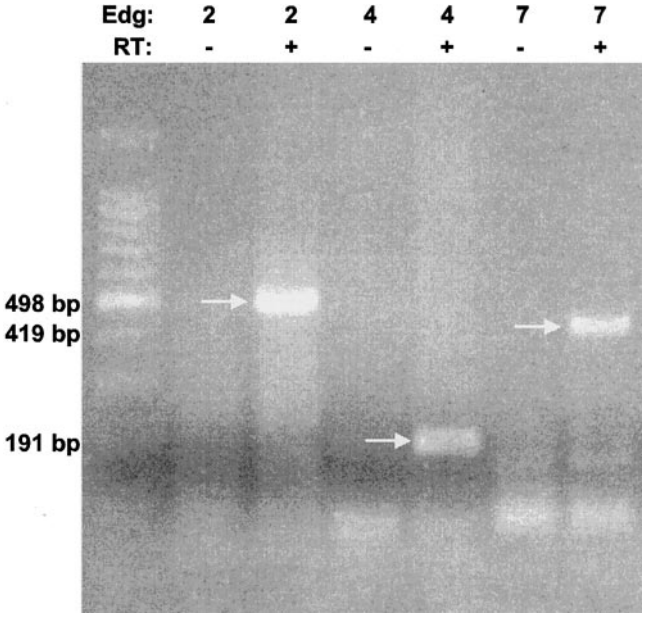

FIGURE 12. RT-PCR indicated the presence of mRNA for the three LPA receptor subtypes, Edg2, -4, and -7, in human RPE cells. When reverse transcriptase was included (RT+), bands of appropriate size were observed: Edg 2 at 498 bp, Edg4 at 191 bp, and Edg7 at 419 bp. No bands were observed when reverse transcriptase was omitted (RT−).

cation channels or voltage-gated Ca^{2+} channels. A possible contribution of Ca^{2+} influx through LPA-stimulated cation channels is supported by the inhibition of these channels by Cd^{2+}.[14]

Although influx appeared to contribute to LPA-evoked Ca^{2+} responses, the finding that responses persisted in Ca^{2+}-free medium indicates that they do not require Ca^{2+} influx. In support of a role for release of Ca^{2+} from intracellular stores, depletion of Ca^{2+} stores by prior application of thapsigargin inhibited both ATP- and LPA-evoked Ca^{2+} responses. The ineffectiveness of U73122 and ryanodine in blocking LPA-evoked responses suggests that the mechanism mediating release of Ca^{2+} from intracellular stores is unlikely to involve IP_3 or ryanodine receptors (Figs. 9, 10). Other intracellular Ca^{2+} release messengers that have been described in recent years include nicotinic acid adenine dinucleotide phosphate (NAADP), cyclic ADP ribose, leukotriene B4, and intracellular sphingolipids.[47] It has been shown that activation of Edg4 receptors by LPA stimulates a ryanodine- and IP_3-independent Ca^{2+} release, which requires intracellular production of sphingosine-1-phosphate in human SH-SY5Y neuroblastoma cells.[48,49] Although to our knowledge direct activation of Ca^{2+} release by MAPK has not been described, MAPK stimulates phospholipase A2 to generate sphingosine,[50] which may in turn lead to increased sphingosine-1-phosphate levels. The possibility of sphingosine-1-phosphate mediating effects of LPA on Ca^{2+} release in RPE cells is an exciting direction for future research.

Genistein significantly inhibited the LPA-evoked cation current in rat RPE cells, but not the LPA-evoked Ca^{2+} response in human RPE cells (Figs. 3, 11). In addition to the possibility of species differences, one way to account for these results is that cation channels are downstream in the signaling cascade from the calcium response, perhaps functioning as store-operated cation channels activated on depletion of intracellular Ca^{2+} stores.[47] Alternatively, the ability of genistein to inhibit the LPA-activated cation current more strongly than the LPA-evoked Ca^{2+} response may reflect LPA-activation of receptor tyrosine kinase (RTK) signaling pathways that target the cation channels independent of MAPK. In a human fibroblast cell line, in which activation of MAPK occurs independent of RTK activities, LPA can activate an RTK- phosphoinositide 3-kinase signaling pathway.[51] These hypothetical pathways by which LPA may regulate cation channels and intracellular Ca^{2+} levels in RPE cells are illustrated schematically in Figure 14.

In addition to PTx-sensitive responses, there also appear to be PTx-insensitive components to LPA responses, including inhibition of cAMP accumulation in some cells (Fig. 5) and K^+ current activation.[14] PTx-insensitive inhibition of cAMP accumulation does not appear to involve activation of a phosphodiesterase, because it is not blocked by isobutylmethylxanthine

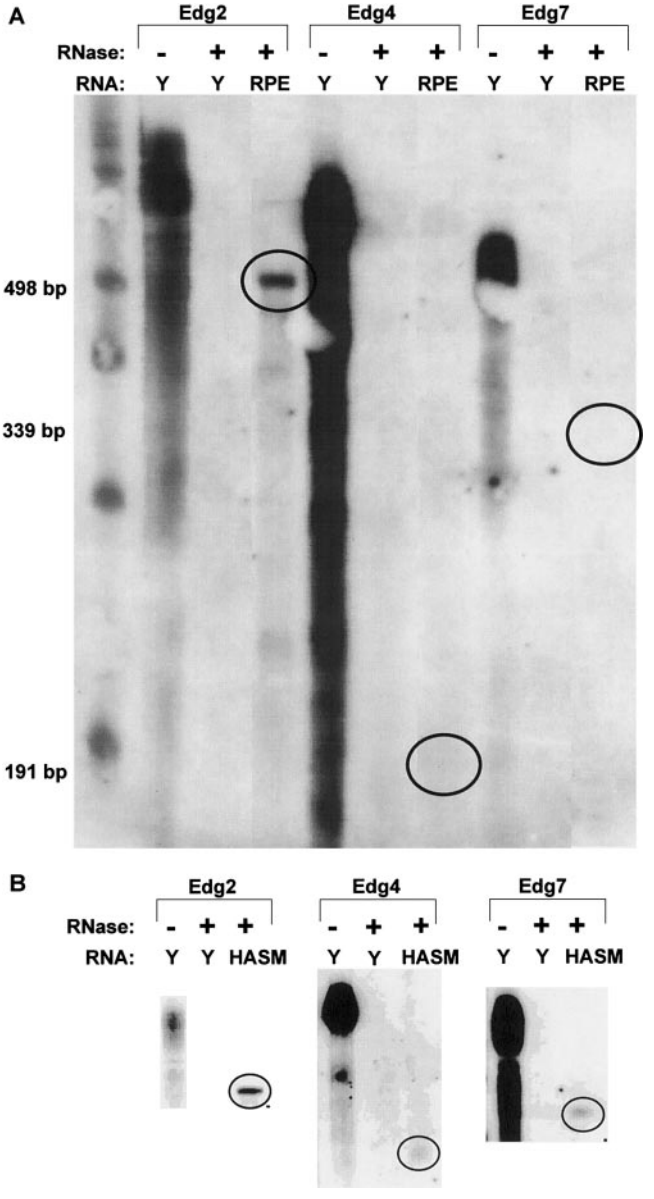

FIGURE 13. RPA indicated high expression of Edg2 receptor RNA. (**A**) When 10 μg of RNA from human RPE was used, a 498-bp band representing Edg-2 was clearly visible, whereas 191- and 339-bp bands corresponding to Edg4 and Edg7, respectively, were not detected (*circles*). The undigested antisense probes from yeast (Y) RNA for all three receptors produced very strong bands (RNase−) but these bands disappeared after digestion with RNase (RNase+). (**B**) In human airway smooth muscle (HASM) cells, RPAs yielded bands for all three receptors (*circles*).

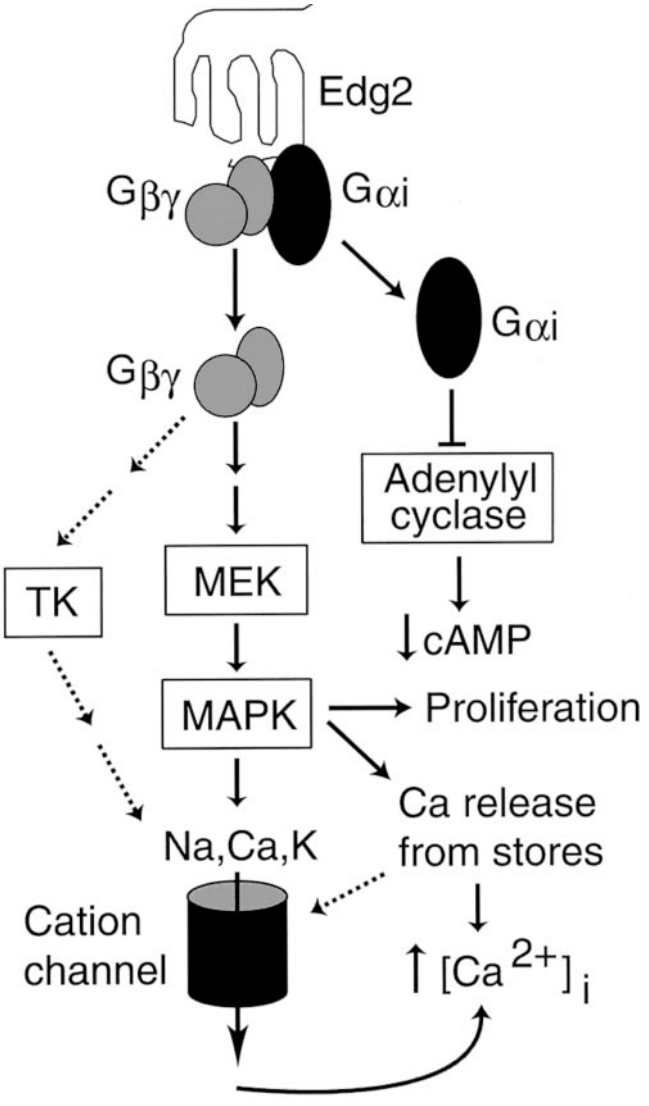

FIGURE 14. G_i-coupled signaling pathways suggested by the present results. Binding of LPA to its receptor, probably Edg2, activates the G-protein. Activation of $G_{\alpha i}$ inhibits adenylyl cyclase to reduce cAMP levels, whereas $G_{\beta\gamma}$ activation initiates a signaling cascade resulting in activation of MEK and MAPK. MAPK, perhaps through activation of intermediary enzymes, stimulated cell proliferation, cation channel activity, and release of Ca^{2+} from intracellular stores. Ca^{2+} influx, probably through LPA-activated cation channels, also contributes to the observed increase in intracellular Ca^{2+}. *Dashed arrows* denote the more speculative possibilities that the LPA-sensitive cation channel may be activated by depletion of intracellular Ca^{2+}, or that tyrosine kinase (TK) may activate other signaling pathways independent of MAPK.

(IBMX). Although we cannot rule out the possibility that differences in PTx uptake and sensitivity of G-protein block in cells from different donor eyes may account for the failure of PTx to inhibit cAMP accumulation in all cells, these differences are unlikely to explain the insensitivity of K^+ currents to PTx, because cation currents were significantly inhibited by PTx pretreatment in the same cells.[14] Activation of PTx-insensitive G proteins in RPE cells by LPA does not appear to involve G_q-coupled PLC activation, because LPA did not stimulate PI turnover (Fig. 7) and, unlike the ATP response, the LPA-evoked Ca^{2+} increase was not blocked by the phospholipase C blocker U73122 (Fig. 9). It is plausible that LPA may activate $G_{12/13}$ in RPE cells, because LPA stimulates RPE cell chemotaxis,[15] and activation of Rho by $G_{12/13}$ can cause, among other things, cell migration.[52]

We used ATP as a positive control for Ca^{2+} and IP_3 studies. The finding that ATP stimulated Ca^{2+} increases in RPE cells is consistent with the results of several previous studies.[24,42–44] The receptor subtype responsible for these responses appears to be the P_2Y_2 purinergic receptor.[24] In endothelial cells, P_2Y_2 receptors stimulate phospholipase C, increasing IP production leading to release of Ca^{2+} from IP_3-sensitive stores.[41,53] A similar pathway seems to operate in RPE cells, because we found that ATP stimulated IP production, inhibition of phospholipase C inhibited ATP-induced Ca^{2+} responses, and depletion of intracellular Ca^{2+} stores with thapsigargin diminished ATP responses.

It has been suggested that phospholipid growth factors such as LPA participate in development, wound healing, and tissue regeneration.[1] The physiological or pathophysiological roles for LPA receptors in RPE cells remain unclear. The RPE forms part of the blood–retinal barrier and contributes to homeostatic maintenance of photoreceptors. Activation of cation and K^+ currents would be expected to alter ion transport across the RPE. Changes in MAPK and cAMP-dependent protein kinase activity may also regulate the activity of other ion channels or transporters in RPE cells. As in other cell types, the activation of cation and K^+ currents by LPA in RPE cells is accompanied by stimulation of mitogenesis.[54] The ability of LPA to stimulate proliferation and chemotaxis may contribute to wound healing and the exaggerated wound healing response that underlies proliferative vitreoretinopathy. Further studies of LPA's effects on RPE cells and the pathways involved may shed new light on the role of LPA in the eye and on mechanisms involved in physiological and pathologic regulation of RPE function.

References

1. An S, Goetzl EJ, Lee H. Signaling mechanisms and molecular characteristics of G protein-coupled receptors for lysophosphatidic acid and sphingosine 1-phosphate. *J Cell Biochem.* 1998;30–31(suppl):147–157.
2. Contos JJ, Ishii I, Chun J. Lysophosphatidic acid receptors. *Mol Pharmacol.* 2000;58:1188–1196.
3. Goetzl EJ, An S. Diversity of cellular receptors and functions for the lysophospholipid growth factors lysophosphatidic acid and sphingosine 1-phosphate. *FASEB J.* 1998;12:1589–1598.
4. Tigyi G, Fischer DJ, Baker D, et al. Pharmacological characterization of phospholipid growth-factor receptors. *Ann NY Acad Sci.* 2000;905:34–53.
5. Pages C, Simon M, Valet P, Saulnier-Blache JS. Lysophosphatidic acid synthesis and release. *Prostaglandins.* 2001;64:1–10.
6. Liliom K, Guan Z, Tseng JL, Desiderio DM, Tigyi G, Watsky MA. Growth factor-like phospholipids generated after corneal injury. *Am J Physiol.* 1998;274:C1065–C1074.
7. Westermann AM, Havik E, Postma FR, et al. Malignant effusions contain lysophosphatidic acid (LPA)-like activity. *Ann Oncol.* 1998;9:437–442.
8. Watsky MA. Lysophosphatidic acid, serum, and hyposmolarity activate Cl^- currents in corneal keratocytes. *Am J Physiol.* 1995;269:C1385–C1393.
9. Roy P, Petroll WM, Cavanagh HD, Jester JV. Exertion of tractional force requires the coordinated up-regulation of cell contractility and adhesion. *Cell Motil Cytoskeleton.* 1999;43:23–34.
10. Ohata H, Tanaka K, Aizawa H, Ao Y, Iijima T, Momose K. Lysophosphatidic acid sensitises Ca^{2+} influx through mechanosensitive ion channels in cultured lens epithelial cells. *Cell Signal.* 1997;9:609–616.
11. Nakamura M, Nagano T, Chikama T, Nishida T. Role of the small GTP-binding protein rho in epithelial cell migration in the rabbit cornea. *Invest Ophthalmol Vis Sci.* 2001;42:941–947.

12. Zhou WL, Sugioka M, Yamashita M. Lysophosphatidic acid-induced Ca^{2+} mobilization in the neural retina of chick embryo. *J Neurobiol.* 1999;41:495–504.
13. Kusaka S, Kapousta-Bruneau N, Green DG, Puro DG. Serum-induced changes in the physiology of mammalian retinal glial cells: role of lysophosphatidic acid. *J Physiol (Lond).* 1998;506:445–458.
14. Thoreson WB, Chacko DM. Lysophosphatidic acid stimulates two ion currents in cultured human retinal pigment epithelial cells. *Exp Eye Res.* 1997;65:7–14.
15. Thoreson WB, Khandalavala BN, Manahan RG, Liu JL, Polyak IA, Chacko DM. Lysophosphatidic acid stimulates proliferation of human retinal pigment epithelial cells. *Curr Eye Res.* 1997;16:698–702.
16. An S, Bleu T, Hallmark OG, Goetzl EJ. Characterization of a novel subtype of human G protein-coupled receptor for lysophosphatidic acid. *J Biol Chem.* 1998;273:7906–7910.
17. An S, Dickens MA, Bleu T, Hallmark OG, Goetzl EJ. Molecular cloning of the human Edg2 protein and its identification as a functional cellular receptor for lysophosphatidic acid. *Biochem Biophys Res Commun.* 1997;231:619–622.
18. An S, Bleu T, Huang W, Hallmark OG, Coughlin SR, Goetzl EJ. Identification of cDNAs encoding two G protein-coupled receptors for lysosphingolipids. *FEBS Lett.* 1997;417:279–282.
19. Bandoh K, Aoki J, Hosono H, et al. Molecular cloning and characterization of a novel human G-protein-coupled receptor, EDG7, for lysophosphatidic acid. *J Biol Chem.* 1999;274:27776–27785.
20. Guo Z, Liliom K, Fischer DJ, et al. Molecular cloning of a high-affinity receptor for the growth factor-like lipid mediator lysophosphatidic acid from Xenopus oocytes. *Proc Natl Acad Sci USA.* 1996;93:14367–14372.
21. Hecht JH, Weiner JA, Post SR, Chun J. Ventricular zone gene-1 (*vzg-1*) encodes a lysophosphatidic acid receptor expressed in neurogenic regions of the developing cerebral cortex. *J Cell Biol.* 1996;135:1071–1083.
22. Im DS, Heise CE, Ancellin N, et al. Characterization of a novel sphingosine 1-phosphate receptor, Edg-8. *J Biol Chem.* 2000;275:14281–14286.
23. Im DS, Heise CE, Harding MA, et al. Molecular cloning and characterization of a lysophosphatidic acid receptor, Edg-7, expressed in prostate. *Mol Pharmacol.* 2000;57:753–759.
24. Sullivan DM, Erb L, Anglade E, WeismanGA, Turner JT, Csaky KG. Identification and characterization of P2Y2 nucleotide receptors in human retinal pigment epithelial cells. *J Neurosci Res.* 1997;49:43–52.
25. Poyer JF, Ryan JS, Kelly ME. G protein-mediated activation of a nonspecific cation current in cultured rat retinal pigment epithelial cells. *J Membr Biol.* 1996;153:13–26.
26. Ryan JS, Kelly ME. Activation of a nonspecific cation current in rat cultured retinal pigment epithelial cells: involvement of a $G_{(alpha\ i)}$ subunit protein and the mitogen-activated protein kinase signalling pathway. *Br J Pharmacol.* 1998;124:1115–1122.
27. Wang N, Koutz CA, Anderson RE. A method for the isolation of retinal pigment epithelial cells from adult rats. *Invest Ophthalmol Vis Sci.* 1993;34:101–107.
28. Neill JM, Barnstable CJ. Expression of the cell surface antigens RET-PE2 and N-CAM by rat retinal pigment epithelial cells during development and in tissue culture. *Exp Eye Res.* 1990;51:573–583.
29. Hamill OP, Marty A, Neher E, Sakmann B, Sigworth FJ. Improved patch-clamp techniques for high-resolution current recording from cells and cell-free membrane patches. *Pflugers Arch.* 1981;391:85–100.
30. Levis RA, Rae JL. Low-noise patch-clamp techniques. *Methods Enzymol.* 1998;293:218–266.
31. Barry PH, Lynch JW. Liquid junction potentials and small cell effects in patch-clamp analysis. *J Membr Biol.* 1991;121:101–117.
32. Lowry OH, Rosenbrough NJ, Farr AL, Randall RJ. Protein measurement with Folin phenol reagent. *J Biol Chem.* 1951;193:265–275.
33. Kreps DM, Whittle SM, Hoffman JM, Toews ML. Lysophosphatidic acid mimics serum-induced sensitization of cyclic AMP accumulation. *FASEB J.* 1993;7:1376–1380.
34. Nogami M, Whittle SM, Romberger DJ, Rennard SI, Toews ML. Lysophosphatidic acid regulation of cyclic AMP accumulation in cultured human airway smooth muscle cells. *Mol Pharmacol.* 1995;48:766–773.
35. Nakahata N, Martin MW, Hughes AR, Hepler JR, Harden TK. H1-histamine receptors on human astrocytoma cells. *Mol Pharmacol.* 1986;29:188–195.
36. Zhu SJ, Cerutis DR, Anderson JL, Toews ML. Regulation of hamster alpha 1B-adrenoceptors expressed in Chinese hamster ovary cells. *Eur J Pharmacol.* 1996;299:205–212.
37. Grynkiewicz G, Poenie M, Tsien RY. A new generation of Ca^{2+} indicators with greatly improved fluorescence properties. *J Biol Chem.* 1985;260:3440–3450.
38. Crepel V, Panenka W, Kelly ME, MacVicar BA. Mitogen-activated protein and tyrosine kinases in the activation of astrocyte volume-activated chloride current. *J Neurosci.* 1998;18:1196–1206.
39. Schliess F, Sinning R, Fischer R, Schmalenbach C, Haussinger D. Calcium-dependent activation of Erk-1 and Erk-2 after hypo-osmotic astrocyte swelling. *Biochem J.* 1996;320:167–171.
40. Chen WC, Chen CC. ATP-induced arachidonic acid release in cultured astrocytes is mediated by G_i protein coupled P2Y1 and P2Y2 receptors. *Glia.* 1998;22:360–370.
41. Pirotton S, Communi D, Motte S, Janssens R, Boeynaems JM. Endothelial P2-purinoceptors: subtypes and signal transduction. *J Auton Pharmacol.* 1996;16:353–356.
42. Peterson WM, Meggyesy C, Yu K, Miller SS. Extracellular ATP activates calcium signaling, ion, and fluid transport in retinal pigment epithelium. *J Neurosci.* 1997;17:2324–2337.
43. Ryan JS, Baldridge WH, Kelly ME. Purinergic regulation of cation conductances and intracellular Ca^{2+} in cultured rat retinal pigment epithelial cells. *J Physiol (Lond).* 1999;520:745–759.
44. Stalmans P, Himpens B. Confocal imaging of Ca^{2+} signaling in cultured rat retinal pigment epithelial cells during mechanical and pharmacologic stimulation. *Invest Ophthalmol Vis Sci.* 1997;38:176–187.
45. Strauss O, Mergler S, Wiederholt M. Regulation of L-type calcium channels by protein tyrosine kinase and protein kinase C in cultured rat and human retinal pigment epithelial cells. *FASEB J.* 1997;11:859–867.
46. Ueda Y, Steinberg RH. Dihydropyridine-sensitive calcium currents in freshly isolated human and monkey retinal pigment epithelial cells. *Invest Ophthalmol Vis Sci.* 1995;36:373–380.
47. Bootman MD, Collins TJ, Peppiatt CM, et al. Calcium signaling: an overview. *Semin Cell Dev Biol.* 2001;12:3–10.
48. Young KW, Bootman MD, Channing DR, et al. Lysophosphatidic acid-induced Ca^{2+} mobilization requires intracellular sphingosine-1 phosphate production: potential involvement of endogenous Edg-4 receptors. *J Biol Chem.* 2000;275:38532–38539.
49. Young KW, Challiss RAJ, Nahorski SR, Mackrill JJ. Lysophosphatidic acid-mediated Ca^{2+} mobilization in human SH-SY5Y neuroblastoma cells is independent of phosphoinositide signaling, but dependent on sphingosine kinase activation. *Biochem J.* 1999;343:45–52.
50. Lin LL, Wartmann M, Lin AY, Knopf JL, Seth A, Davis RJ. cPLA2 is phosphorylated and activated by MAP kinase. *Cell* 1993;72:269–278.
51. Laffargue M, Raynal P, Yart A, et al. An epidermal growth factor receptor/Gab1 signaling pathway is required for activation of phosphoinositide 3-kinase by lysophosphatidic acid. *J Biol Chem.* 1999;274:32835–32841.
52. Sah VP, Seasholtz TM, Sagi SA, Brown JH. The role of Rho in G protein-coupled receptor signal transduction. *Annu Rev Pharmacol Toxicol.* 2000;40:459–489.
53. Viana F, de Smedt H, Droogmans G, Nilius B. Calcium signalling through nucleotide receptor P2Y2 in cultured human vascular endothelium. *Cell Calcium.* 1998;24:117–127.
54. Nilius B, Droogmans B. Ion channels and their functional role in vascular endothelium. *Physiol Rev.* 2001;81:1415–1459.